Published in final edited form as:
Cell. 2012 March 30; 149(1): 188–201. doi:10.1016/j.cell.2012.01.046.

Young Dentate Granule Cells Mediate Pattern Separation whereas Old Granule Cells Contribute to Pattern Completion

Toshiaki Nakashiba[1], **Jesse D. Cushman**[2], **Kenneth A. Pelkey**[3], **Sophie Renaudineau**[1], **Derek L. Buhl**[1], **Thomas J. McHugh**[1,*], **Vanessa Rodriguez Barrera**[2], **Ramesh Chittajallu**[3], **Keisuke S. Iwamoto**[4], **Chris J. McBain**[3], **Michael S. Fanselow**[2], and **Susumu Tonegawa**[1,**]

[1]RIKEN-MIT Center for Neural Circuit Genetics at The Picower Institute for Learning and Memory, Department of Biology and Department of Brain and Cognitive Sciences, Massachusetts Institute of Technology, Cambridge, MA 02139, USA

[2]Department of Psychology, Department of Psychiatry and Biobehavioral Sciences, University of California, Los Angeles, Los Angeles, CA 90095, USA

[3]Laboratory of Cellular and Synaptic Neurophysiology, Eunice Kennedy Shriver National Institute of Child Health and Human Development, National Institutes of Health, Bethesda, MD 20892, USA

[4]Department of Radiation Oncology, David Geffen School of Medicine, University of California, Los Angeles, Los Angeles, CA 90095, USA

Summary

Adult-born granule cells (GCs), a minor population of cells in the hippocampal dentate gyrus, are highly active during the first few weeks following functional integration into the neuronal network (young GCs), distinguishing them from less active older adult-born GCs and the major population of dentate GCs generated developmentally (together, old GCs). We created a transgenic mouse in which output of old GCs was specifically inhibited while leaving a substantial portion of young GCs intact. These mice exhibited enhanced or normal pattern separation between similar contexts that was reduced following removal of young GCs by X-ray irradiation. Furthermore, mutant mice exhibited deficits in rapid pattern completion. Therefore, pattern separation of similar contexts requires adult-born young GCs while old GCs are unnecessary, whereas older GCs contribute to the rapid recall by pattern completion. Our data suggest that as adult-born GCs age, their function switches from pattern separation to rapid pattern completion.

Introduction

The hippocampus plays a crucial role in episodic memory (Scoville and Milner, 1957; Burgess et al., 2002; Squire et al., 2004). It allows the formation of distinct memories of similar episodes by generating distinct representations of the temporal and spatial relationships comprising the events (pattern separation). This ability of the hippocampus is critical because many episodes we experience daily have similarities, but it is often

**To whom correspondence should be addressed: tonegawa@mit.edu.
*Present address: RIKEN Brain Science Institute, 2-1 Hirosawa, Wako-Shi, Saitama 351-0198, Japan

important to memorize distinct features of a particular episode. The hippocampus is also involved in the recall of previously acquired memories by reactivating the full representations of those memories using partial information as recall cues (pattern completion). This ability of the hippocampus is also important because in real life, specific episodes are rarely replicated in full.

These mnemonic requirements have been suggested to be subserved by specific hippocampal subregions and circuits (Figure 1A). For pattern completion, synaptic transmission and plasticity in the recurrent network of CA3 has been proposed by models to play a crucial role on a theoretical basis (Marr, 1971; McNaughton and Morris, 1987; O'Reilly and McClelland, 1994; Treves and Rolls, 1994; Hasselmo et al., 1995), which has been supported by the targeted manipulation of NMDA receptors in CA3 (Nakazawa et al., 2002). Conversely, synaptic transmission and plasticity in the feed-forward pathway from the entorhinal cortex (EC) → dentate gyrus (DG) → CA3 has been implicated in pattern separation based on the spatial and temporal segregation of the initially overlapping EC memory engrams (Marr, 1971; McNaughton and Morris, 1987; O'Reilly and McClelland, 1994; Treves and Rolls, 1994; Leutgeb et al., 2007; Bakker et al., 2008). This hypothesis has been supported by impairments observed in rodents with DG lesions (Gilbert et al., 2001; Hunsaker and Kesner, 2008) as well as mice with a targeted deletion of NMDA receptors in DG granule cells (GCs) (McHugh et al., 2007). These theoretical and experimental studies, however, did not consider the heterogeneity of DG GCs where most GCs (~95%) are generated early during development and do not divide thereafter throughout the animal's life (developmentally born neurons) (Schlessinger et al., 1975; Altman and Bayer, 1990). However, the DG also contains neural progenitor cells that generate GCs throughout life (adult-born neurons), which compose the remaining ~5% of the total GCs in adult animals (Altman and Das, 1965; Eriksson et al., 1998; Gould et al., 1999; Imayoshi et al., 2008). Recently, mice with reduced adult-born cells were shown to exhibit a deficit in pattern separation (Clelland et al., 2009; Scobie et al., 2009; Tronel et al., 2010), whereas mice with augmented adult neurogenesis were shown to have enhanced pattern separation (Creer et al., 2010; Sahay et al., 2011). These studies left unanswered the function of the vast majority of the GCs generated developmentally. Are they also involved in pattern separation as the theories and earlier experiments suggested? Another unanswered question concerns with the age of adult-born GCs. These cells are highly active during the first few weeks following functional integration into the neuronal network (young GCs; Schmidt-Hieber et al., 2004; Ge et al., 2007) but become less active thereafter and functionally indistinguishable from the old developmentally born GCs (together, old GCs; Laplagne et al., 2006). The previous studies did not specify which of the two subsets of adult-born GCs (young or old, or both) are responsible for pattern separation.

To investigate these issues, we created a transgenic mouse in which output of old GCs was specifically inhibited by the tetanus toxin (TeTX) while leaving young GCs (up to 3-4 week-old) intact and examined the pattern separation capability of these mice using context- or space-discriminating memory tasks. These mice exhibited normal or enhanced pattern separation capability between similar contexts that was significantly reduced following removal of young GCs by X-ray irradiation. Contrary to expectations, mutant mice (no X-ray irradiation) displayed deficits in rapid pattern completion-mediated memory recall.

Results

Generation of triple-transgenic mice

Triple-transgenic DG-TeTX mouse and the triple-transgenic DG-GFP mouse were generated using the DICE-K method (Nakashiba et al., 2008) (Figure 1B). In the model mouse raised on Dox followed by a 2-week Dox withdrawal, GFP was expressed robustly and exclusively

in the DG throughout the septo-temporal axis (Figure S1A and B). GFP expression was detected in the DG GC layer, the DG molecular layer and the CA3 s. lucidum, corresponding to the location of GC dendrites and MFs, respectively (Figure 1C to 1E). GFP expression was repressed under Dox-on conditions (Figure 1F), activated under Dox-on-off conditions (Figure 1G) and re-repressed under Dox-on-off-on conditions (Figure 1H), in which mice were returned to a Dox diet for 3 weeks after 2 weeks of Dox withdrawal.

MF synaptic transmission is blocked in DG-TeTX mice

VAMP2's immunoreactivity (IR) can be used as a criterion for transmission at MF-CA3 synapses. VAMP2 IR patterns were indistinguishable between the DG-TeTX and control mice (all control mice are of the Tg1xTg3-TeTX genotype) kept on Dox (Figure 1I and J). After 4 weeks of Dox withdrawal, VAMP2 IR was greatly reduced selectively in the s. lucidum in DG-TeTX mice (Figure 1K), suggesting an inhibition of synaptic transmission at MF terminals. VAMP2 IR was restored to control levels following a 4-week Dox-on period (Figure 1L).

Synaptic transmission at MF, perforant path (PP) and recurrent (RC) inputs in slices from repressed DG-TeTX and control mice were indistinguishable (Figure 2A, C and D). In contrast, slices from activated DG-TeTX mice exhibited severely impaired MF transmission but normal PP and RC transmission (Figure 2A, C and D). Importantly, MF excitability was comparable between control, repressed and activated DG-TeTX mice (Figure S2), confirming that the impaired MF transmission observed in the DG-TeTX mice reflects a deficit in release rather than inefficient fiber stimulation. Even in the presence of forskolin to maximally enhance release probability (Weisskopf et al., 1994), MF transmission remained barely detectable in slices from activated DG-TeTX mice, in contrast to the robust potentiation observed in slices from control and repressed DG-TeTX mice (Figure 2B). As with VAMP2 IR, MF transmission was completely restored in slices from re-repressed DG-TeTX mice (Figure 2A and B). Considered together, the *ex vivo* VAMP2 IR and *in vitro* field recording data indicate that MF synaptic transmission in DG-TeTX mice is robustly inhibited by the loss of vesicle fusion selectively at MF terminals in an inducible and reversible manner. Importantly, no detectable abnormalities were found in the cytoarchitecture of MF projections or the hippocampus in activated DG-TeTX mice (Figure S1C and D).

MF synapses of young adult-born GCs are intact in DG-TeTX mice

The generation and survival of adult-born GCs were normal in activated adult DG-TeTX mice (Figure S3A to C). Moreover, the differentiation of neural progenitor cells in activated DG-TeTX mice produced normal proportions of GCs and glia (Figure S3D to G). A genetically engineered Moloney viral vector (Figure 3A) was injected into the DG of activated DG-TeTX mice and control littermates to selectively label MF boutons from adult-born GCs (van Praag et al., 2002) and examine whether the transmission at these synapses are inhibited (Figure 3B). Three weeks after the viral injection (Figure 3C and D), numerous mCherry-fused VAMP2-positive puncta (mCheV2, red) appeared in CA3 s. lucidum (where MFs should synapse onto CA3 cells). These puncta were superimposed nearly perfectly with GFP-fused Synaptophysin (SypGFP, green) in both activated DG-TeTX mice and control littermates, with no discernable difference between the two genotypes. Conversely, 6 weeks after the injection (Figure 3E), the proportion of SypGFP-positive puncta colocalized with mCheV2 was substantially reduced in only the activated DG-TeTX mice. A gradual decrease of this proportion over the ages of the adult-born GCs was observed (Figure 3F), suggesting that synaptic transmission at MF terminals of young adult-born GCs (up to 3 weeks old) was relatively intact, although it gradually decreased as the cells became older (Figure 3F). This conclusion was supported by the lack of GFP expression in the adult-born

doublecortin (DCX)-positive GCs (a marker for up to 3-week-old cells) (Nacher et al., 2001; Snyder et al., 2009) in the model DG-GFP mice (Figure 3G to K). Additional experiments using wheat germ agglutinin (WGA), a synaptic vesicle fusion-dependent anterograde trans-synaptic marker (Tabuchi et al., 2000; Braz et al., 2002), demonstrated that synaptic transmission from 4-week-old adult-born GCs was intact, at least in the hilar region, in activated DG-TeTX mice (Figure S3H to L).

Young adult-born GCs in DG-TeTX mice receive functional synaptic inputs and their functions are unaffected by the TeTX manipulation

To examine synaptic inputs to young (3-week-old) adult-born GCs, we injected another Moloney virus (Figure 4A, Virus 1A) and an engineered rabies virus (Figure 4B, Virus 2; Wickersham et al., 2007) into the DG of activated DG-TeTX mice and control littermates (see Experimental Procedures). In a control hippocampal section, nearly all GFP-positive (i.e., TVA- and rabies G-positive) young adult-born GCs had RFP signal derived from Virus 2 as a result of direct interaction between EnvA and TVA (Figure 4C). With the complementation of rabies G in the GFP-positive GCs, monosynaptic retrograde labeling occurred extensively in the hilar region and sparsely in CA3, where the RFP signal never overlapped with GFP, excluding the possibility of direct Virus 2 infection into those cells (Figure 4C). RFP signal was also detected in NeuN-positive neurons of EC superficial layer II with dendrites extending toward layer I (Figure 4E and G). RFP signal was rarely detected in cells other than GFP-positive GCs when rabies G was not provided by a Moloney virus (Figure 4A, Virus 1B), further confirming the specificity of retrograde labeling (Figure 4D and F). In activated DG-TeTX mice, there was no discernable difference from control mice in brain areas where cells were retrogradely labeled from young 3-week-old adult-born GCs (Figure 4C, E and G), indicating young adult-born GCs in DG-TeTX mice receive synaptic inputs.

We compared the intrinsic membrane and synaptic properties of young adult-born GCs in control and activated DG-TeTX mice. Mice (3-4 months old) were infected with Moloney virus encoding GFP and sacrificed 3-4 weeks later for whole-cell patch clamp recordings from GFP-labeled GCs in acute hippocampal slices (Figure 2E to I). No genotype-specific differences were observed between GFP-labeled GCs for any of the basic membrane and spiking properties including resting membrane potential, input resistance, membrane time constant and spike frequency/duration (Figure 2E and Table S1). GFP-labeled cells received both GABAergic inhibitory and glutamatergic excitatory synaptic input (Figure 2F, G and Table S1), indicating that the synapses observed with rabies virus (Figure 4) were functional. Importantly, comparison of control and DG-TeTX young adult-born GCs revealed no differences in any of the synaptic properties assayed including inhibitory/excitatory postsynaptic current kinetics, AMPA/NMDA ratios and short- or long-term synaptic plasticity at perforant path inputs (Figure 2H, I and Table S1). Together, these findings confirm that adult-born GCs are synaptically integrated into the entorhinal-hippocampal circuitry by 3-4 weeks of age and that blockade of transmission in the developmentally born GCs does not alter the electrophysiological and synaptic properties of young adult-born GCs.

Contextual discrimination is enhanced in DG-TeTX mice for highly similar context pair

Activated DG-TeTX mice did not exhibit detectable abnormalities in anxiety, locomotor activity, motor coordination or pain sensitivity (Figure S5). The activated DG-TeTX mice froze similar to control mice (Figure 5A, ANOVA, genotype; $F_{(1,22)}$=0.145, p= 0.707) in a contextual fear conditioning and exhibited no deficit in distinguishing a pair of relatively distinct contexts, A and D, located in different rooms (Figure 5B, ANOVA, context, $F_{(1,22)}$=107.13, p< 0.0001; genotype, $F_{(1,22)}$=0.155, p=0.698; context × genotype,

$F_{(1,22)}$=2.145, p= 0.157). We then subjected another cohort to a contextual discrimination fear conditioning (McHugh et al., 2007) in which mice learned to discriminate a pair of very similar contexts located in the same room over repeated trials with a single footshock in one of the contexts (shock context; A). The other context (safe context; B) shared nearly all features with A, except that the sidewalls in B sloped inward at a 60° angle from the floor. This task, in which DG-NR1 mice are known to be impaired (McHugh et al., 2007), requires mice to respond to two similar patterns based on their memory of previous experiences with those patterns. On the first 3 days, the mice were placed only into A, receiving a footshock after 180 s. Freezing levels were assessed for the first 3 min before shock delivery (Figure 5C). During conditioning, activated DG-TeTX mice acquired fear memory to A similar to control mice (Figure 5C, ANOVA, genotype; $F_{(1,22)}$=0.140, p=0.712). Context specificity was tested on days 4 and 5, when the mice of each genotype were divided into two groups. One group visited A then B on day 4 and B then A on day 5, whereas the other group visited the contexts in the opposite order. Neither group received a shock in A or B (Figure 5D). Mice froze somewhat more in the shock context (A) than the nonshocked context (B). Both genotypes showed robust and equivalent generalization between contexts, and no discernable differences in freezing were observed (Figure 5D, ANOVA, context, $F_{(1,22)}$=4.867, p<0.04; genotype, $F_{(1,22)}$=2.162, p=0.156; context × genotype, $F_{(1,22)}$=1.023, p=0.323). The mice were subsequently trained to discriminate these contexts by visiting the two contexts daily for 12 days, always receiving a footshock 180 s after being placed in A but not B (Figure 5E). Discrimination training was analyzed for each trial block within each genotype using Scheffé's method. As shown in Figure 5F and G, only activated DG-TeTX mice exhibited significant discrimination across all trial blocks, whereas controls did not acquire significant discrimination until the final two trial blocks. Thus, the loss of MF transmission in developmentally born GCs and older adult-born GCs resulted in *no* deficit in the discrimination of highly similar contexts but rather an enhanced discrimination compared to control mice.

Contextual discrimination depends on young adult-born GCs both in DG-TeTX and control mice

We next ablated adult-born DG GCs by irradiating activated DG-TeTX mice and control littermates with X-ray (Santarelli et al., 2003; Figure 5H, I and O) and subjected the irradiated (IR) and sham-operated (Sham) mice to contextual discrimination fear conditioning (Figure 5J to N). Given that the previously used highly similar context pair (A vs. B) was difficult for control mice to discriminate (Figure 5F), we chose to use a more distinct yet similar context pair to test the role of adult-born GCs in pattern separation, thus allowing for a clearer detection of potential discrimination deficits. The context pair used (A vs. C) was located in the same room and differed in odor and background noise, in addition to differing sidewalls (which were the only feature that differed between the highly similar pair, A and B). All four groups acquired a similar fear memory to A (Figure 5J, ANOVA, genotype $F_{(1,52)}$=0.314, p=0.578; irradiation: $F_{(1,52)}$=0.350, p=0.350; genotype × irradiation: $F_{(1,52)}$=2.487, p=0.121) and showed strong generalization to C over the 2-day generalization test (ANOVA, context: $F_{(1,52)}$=22.578, p < 0.001). However, DG-TeTX mice showed a slight, but significant, elevation in generalization to context C, (ANOVA, context × genotype: $F_{(1,52)}$=7.296, p < 0.009) and this was not affected by irradiation (Figure 5K, ANOVA, context × genotype × irradiation interaction: $F_{(1,52)}$=0.725, p=0.398). Discrimination training was analyzed again using Scheffé's method. During discrimination trainings (Figure 5L to N), Sham control mice began to discriminate A and C on trial block 2, three blocks earlier than the A vs. B discrimination (Figure 5F). In contrast, IR control mice did not discriminate until trial block 3 (Figure 5M), confirming that adult-born GCs are important for efficient discrimination. The irradiation effect was also observed in activated DG-TeTX mice (Figure 5N). Sham DG-TeTX mice began to discriminate on trial block 3

(one block later than Sham control mice), whereas IR DG-TeTX mice were unable to discriminate until trial block 5, therefore exhibiting the worst discrimination efficiency among the four groups and indicating that young, adult-born GCs in activated DG-TeTX mice are crucial for the contextual discrimination observed in these mice.

Spatial discrimination is normal in DG-TeTX mice

For another test of behavioral discrimination, we used a delayed non-matching to place (DNMP) task in an eight-arm radial maze. Mice with reduced hippocampal adult neurogenesis were previously shown to be impaired in this task when the reward arm was relatively close to the sample arm (Clelland et al., 2009). Conversely, our present data shows that activated DG-TeTX mice made correct choices as efficiently as control mice regardless of the angles separating the sample and reward arms (Figure 6A to C, $p>0.05$ for comparison between genotypes in each separation, t-test), indicating that MF inputs from the vast majority of GCs are dispensable for spatial pattern separation.

Rate remapping in the hippocampus is normal in DG-TeTX mice

To obtain a physiological correlate of the normal spatial discrimination observed in the DG-TeTX mice, we investigated possible changes in the ensemble activity in CA3 and CA1 while animals foraged in a novel arena after exploring a similar but distinct familiar environment set in the same room (Figure 6D to G and Table S2). Neuronal ensembles in the CA3 region of DG-TeTX mice exhibited intact rate remapping between the contexts compared to control animals (Figure 6F, ANOVA, genotype × region, $F_{(1,428)}=0.27$, $p=0.62$; genotype, $F_{(1,428)}=1.66$, $p=0.19$; region, $F_{(1,428)}=13.09$, $p<0.001$; Bonferroni post-test, control CA1 × control CA3, $p<0.05$; DG-TeTX CA1 × DG-TeTX CA3, $p<0.001$). The rate differences in CA3 of both DG-TeTX and control mice were what would have been expected from the formation of an independent representation ($p>0.05$ for control and DG-TeTX, respectively, t-test), but CA1 rate differences were not ($p=0.012$ and $p<0.001$ for control and DG-TeTX, respectively, t-test). Figure 6G shows the cumulative probability histogram for the rate overlap in the CA3 and CA1 regions. Importantly, no genotype-specific differences were observed in either CA3 or CA1 ensembles (Mann-Whitney U-test; $p>0.05$), yet in both genotypes, similar differences were observed between the regions (Mann-Whitney U-test; $p<0.05$ and $p<0.01$, respectively). These physiological data support the behavioral data from the spatial discrimination task and the conclusion that output from the vast majority of DG GCs (i.e., old GCs) is not necessary for spatial pattern separation.

Rapid pattern completion-mediated contextual recall is impaired in DG-TeTX mice

The pre-exposure-dependent contextual fear conditioning paradigm (Fanselow, 1986, 1990) has been used previously to test a rodent's ability to carry out pattern completion-based memory recall (Matus-Amat et al., 2004; Nakashiba et al., 2008). Figure 7A summarizes the protocols for the experimental and control groups (see Experimental Procedures). At the probe test, activated DG-TeTX mice displayed a freezing deficit (Figure 7B, $p<0.01$, t-test) that was likely due to the animals' inability to rapidly (10 s reexposure to a context) recall a full contextual representation previously formed (presumably in CA3) during pre-exposure under normal MF transmission, as the freezing deficit was not present when the context reexposure time was prolonged to 3 min (Figure 7B and C, ANOVA, genotype × time, $F_{(1,115)}=4.647$, $p=0.033$, Bonferroni post-test, $p>0.05$ between genotypes in Figure 7C). The freezing deficit was also not seen in DG-TeTX mice when conditioning occurred under the Dox-on condition (Figure 7B and D, ANOVA, genotype × Dox condition, $F_{(1,115)}=4.107$, $p=0.045$, Bonferroni post-test, $p>0.05$ between genotypes in Figure 7D). When the pre-exposures were to a distinct context (Figure 7E), freezing levels were similar to controls not given a footshock (Figure 7F, ANOVA, genotype × condition, $F_{(1,44)}=0.050$, $p=0.8233$; genotype, $F_{(1,44)}=0.019$, $p=0.900$; condition, $F_{(1,44)}=0.161$, $p=0.690$). It is possible that the

contextual memory engram acquired under Dox-on conditions may have been degraded during the subsequent 4-week-long Dox-off period. However, when we measured contextual fear memory in DG-TeTX mice 4 weeks after conditioning we found no genotype-specific difference in freezing levels (Figure S6A and B). These results indicate that MF output from the developmentally born GCs and/or older adult-born GCs is crucially involved in rapid pattern completion-mediated recall of contextual memories.

Rapid pattern completion-mediated spatial recall is impaired in DG-TeTX mice

We next subjected mice to the standard water maze task in which the spatial memory was tested with varying degrees of distal cue availability (Figure 7G and H). DG-TeTX mice learned the location of the hidden platform with kinetics indistinguishable from control littermates under the Dox-on and full-cue conditions (Figure 7I, ANOVA, genotype; $F_{(1, 45)}$=0.027, p=0.870). We did not observe any genotype-specific differences in distance traveled or swim speed (Figure S7A and B). During the probe trials, we used the latency to reach the phantom platform the first time as the measure of rapid memory recall (Nakazawa et al., 2002; Slutsky et al., 2010). In the probe trial conducted at the end of the training session (P1, Dox-on), we did not detect any genotype-specific differences in the latencies (Figure S7C). Following 5 weeks of Dox withdrawal, we subjected the mice to successive probe trials under partial cue conditions, one trial per day. The latencies were significantly longer in activated DG-TeTX mice compared to controls in the one-cue probe trial (P2, Figure 7J and K, p<0.05, t-test), and there were longer, though not significant, latencies for mutants in the two-cue probe trial (P3, Figure 7J and K, p>0.05, t-test). These prolonged latencies were not due to enhanced memory extinction in the mutants because in the full cue probe trial conducted 1 day later, the mutants' latency was comparable to that of controls' (P4, Figure 7J and K), which were not significantly different from the latencies observed in P1 (ANOVA, genotype × probe trials, $F_{(1,45)}$=0.004, p=0.652; genotype, $F_{(1,45)}$=1.203, p=0.279; probe trials, $F_{(1,45)}$=1.986, p=0.166). Furthermore, the longer latencies observed in the mutants under the P2 condition were not due to a deficiency in swimming, as the swim speed in the mutants was similar to that of controls in the full cue probe trial (P4, Figure S7E). The latencies observed in P2, P3 and P4 indicate that while the control mice can recall the memory under partial cue conditions as well as the full cue condition, the mutants' recall ability is sensitive to the extent of cue availability (ANOVA, probe trials, $F_{(2,45)}$=5.777, p=0.004; Bonferroni post-test, p>0.05 for comparison of pairs among P2, P3 and P4 in both genotypes except p<0.01 for P2 vs. P4 in DG-TeTX mice). In the probe trial conducted with none of the four distal cues 1 day after the full cue probe trial (i.e., P5), both genotypes showed similar latencies (Figure S7D). In control mice, the latency in P5 was significantly longer than any of the latencies observed under the other conditions (ANOVA, probe trials, $F_{(3,45)}$=17.92, p<0.0001; Bonferroni post-test, p<0.001 for comparison of P2, P3 or P4 to P5). In contrast, mutants' latency in P5 was indistinguishable from that in P2 (Bonferroni post-test, p>0.05 for P2 vs. P5) but significantly longer than that in P3 or P4 (Bonferroni post-test, p<0.01 for P3 vs. P5, p<0.001 for P4 vs. P5). We also measured the spatial memory under partial cue condition using the 90-s platform occupancy test and found no genotype-specific or cue paucity-dependent deficits (Figure S7F and G). Thus, when sufficient time is allowed, the mutant mice can recall the location of the phantom platform under partial cue condition. These results indicate that the mutants' deficits are in the speed of pattern completion recall rather than in its capacity. Our results suggest that the MF input from old GCs promotes this specific aspect of pattern completion-mediated recall.

DISCUSSION

Because the properties of mutants' dentate GCs are crucial for the interpretation of behavioral and *in vivo* physiological data, we first characterized them using *in vitro*

electrophysiology and cell biology. Our data indicated that in the mutants, transmission is robustly and specifically inhibited at most MF-CA3 synapses under the Dox-off condition (Figure 2). Our data also demonstrated that 3- to 4-week-old adult-born GCs are functionally integrated into the network and that the physiological properties of these adult-born GCs are not affected by lack of MF transmission of the majority of GCs (Figure 2, 3, 4 and S3). The MF-CA3 contacts of the young adult-born GCs, however, gradually declined after 4 weeks of age with about 5% remaining intact at 6 weeks of age (Figure 3E and F). It is known that adult-born dentate GCs are highly excitable and exhibit greater synaptic plasticity compared to the numerically dominant developmentally born (and hence older) GCs (Shmidt-Hieber et al., 2004; Ge et al., 2007) up to ~6 weeks of cellular age and thereafter become less active and indistinguishable from developmentally born GCs (Laplagne et al., 2006). Therefore, it seems that the TeTX manipulation in the DG-TeTX mice spared a substantial portion of the highly excitable and synaptically plastic young adult-born GCs while inhibiting the MF transmission of the most of the developmentally born GCs and less active older (>6 weeks of age) adult-born GCs. In the remaining discussion, we refer the 3- to 4-week–old adult-born GCs as young GCs and the combined developmentally born and older adult-born GCs as old GCs.

Overall, our results indicate that old GCs do not play a critical role in pattern separation between similar environments but are required for attaining a normal level of rapid pattern completion. These findings were unexpected given that previous theoretical and experimental work has suggested that the EC→DG→CA3 pathway is crucial for pattern separation (Marr, 1971; McNaughton and Morris, 1987; Treves and Rolls, 1994; Gilbert et al., 2001; Leutgeb et al., 2007; McHugh et al., 2007; Hunsaker and Kesner, 2008) and has focused less on its contributions to pattern completion, although it has been suggested that pattern completion could be associated with the strengthening of EC→DG synapses (O'Reilly and McClelland, 1994).

Our current study combined with the recent studies focusing on the role of adult-born DG GCs (Clelland et al., 2009; Scobie et al., 2009; Tronel et al., 2010) provide several new concepts and clarifications regarding the function of the EC→DG→CA3 pathway in episodic memory. First, the lack of MF input from old DG GCs did not impair discrimination of similar contexts or spaces (Figure 5C to G and 6A to C), indicating that, under these conditions, neither the greater number nor sparse activity of DG GCs compared to cells in the superficial layers of the EC (Amaral et al., 1990; Jung and McNaughton, 1993), on which most models are based, is sufficient for pattern separation of similar contexts or spaces. This point is important because it is often under these circumstances when we rely on our pattern separation capability for guiding intelligent behavior. Second, we observed a trend indicating old GCs may be involved in the discrimination of relatively distinct contexts (compare Figure 5G and N), suggesting that the spatial and temporal dispersion of memory encoding cells as the information flows from the EC to DG followed by its orthogonalization from DG to CA3 may contribute to pattern separation of relatively distinct contexts. Third, we confirmed by the X-ray irradiation that adult-born DG GCs are crucial for efficient acquisition of the contextual discrimination power in normal mice (Scobie et al., 2009; Tronel et al., 2010; Sahay et al., 2011). Additionally, we demonstrated that it is the young adult-born GCs that were required for the discrimination of similar contexts. Fourth, among the four groups used in the X-ray irradiation experiments, the IR DG-TeTX mice exhibited the lowest efficiency in contextual discrimination (Figure 5M and N). These mice lack functional MF transmission from both developmentally born and adult-born GCs, leaving only the direct perforant path input to CA3 from EC layer II. Thus, our results suggest that this input can not support pattern separation. Finally, regarding the discrepancies between the present work and previous lesion-based studies (Kesner, 2007; Lee and Kesner, 2004), lesions would have damaged the output of both young and old GCs

and therefore would not have permitted the elucidation of their differential roles. Likewise, the contextual discrimination and the rate-remapping deficits observed in DG-NR1 KO mice (McHugh et al., 2007) could be due to the inhibition of synaptic plasticity in young GCs because the POMC promoter is active in these cells (Figure S4; Overstreet et al., 2004).

The enhanced contextual discrimination in activated DG-TeTX mice was observed only when a highly similar pair of contexts was used for contextual fear conditioning (Figure 5F and G). At the moment, we can only speculate how this phenomenon occurred under these conditions. One possibility is that pattern completion and separation are counteractive in control mice and that the deficit in the former led to an enhancement of the latter in mutant mice. This possibility is supported by at least two previous studies. In theoretical models, O'Reilly and McClelland suggested a trade-off between these two mnemonic processes (O'Reilly and McClelland, 1994). In practice, MF boutons from young and old GCs were found to share the same spines of CA3 cells in some cases but synapse separately on different spines from CA3 cells in other cases, suggesting a competition for their targets (Toni et al., 2008). Such a competition or trade-off may be subtly controlled to maintain the optimal balance of separation and completion, and the effect of the reduction of one on the other may not necessarily be revealed in all discrimination tasks. Another possibility for the lack of enhanced discrimination in the radial maze task in our mutants is that discrimination may already be saturated in control mice.

How would MFs from old GCs favor pattern completion while MFs from young GCs promote pattern separation? The core of our hypothesis is that old GCs may tend to lead the system into previously existing CA3 attractor states, whereas younger GCs may help form new attractor states in CA3. Old GCs are likely to have participated in the formation of many memory engrams of numerous past experiences because they have been encoding information throughout the animal's life. These engrams are likely overlapping, perhaps reflecting a high degree of engram overlap in the EC and the high redundancy of the EC→DG connections (Amaral et al., 1990). This is supported by *in vivo* physiology studies showing that it is largely the same GCs, firing at different rates, that allows the DG to generate different representations of similar but distinct environments (Leutgeb et al., 2007). In contrast, young GCs have only recently been incorporated into the functional network, and memory engrams supported by these cells would be greatly limited in their diversity and less likely to overlap than engrams supported by old GCs. When an animal encounters a new experience both old and young GCs would participate in the formation of the new engram in the dentate. These cells would then converge downstream on CA3 to form corresponding engrams. The greater the young GCs contribute to the dentate engram the more distinct the new dentate and CA3 engrams would be, while the old GCs would have an opposite effect. In this process the numerical disadvantage of young GCs over the old GCs may be compensated by the greater excitability and synaptic plasticity of young GCs (Schmidt-Hieber et al., 2004; Ge et al., 2007; Kee et al., 2007; Tashiro et al., 2007), and there may be additional unknown mechanisms that may favor the output of these cells (e.g. differential connection with inhibitory neurons). When two experiences are very similar a greater participation of young GCs would be crucial for separation while the discrimination of a more distinct pair of experiences can be accomplished by greater participation of old GCs. Moreover, our data indicate that for a given pair of experiences the ability to distinguish (separate) can be improved by the repetition of the experiences, presumably via synaptic plasticity (Figure 5 and 6; McHugh et al., 2007).

For pattern completion, information that arrives at the DG via the EC is from partial or degraded recall cues. Such information will activate the previously formed CA3 memory engram more efficiently if it can first activate overlapping DG engrams to which old GCs contributed more than young GCs. Thus, the role of old GCs in pattern completion may be

to rapidly initiate the reactivation of the relevant recurrent network in CA3 that contains the engram for the episode.

Our data indicate that the recall of old memories and the formation of new memories preferentially involve two distinct anatomical substrates consisting of varying subsets of GCs of different ages in the hippocampal DG. Therefore, adult-born GCs likely have a critical period of a few weeks in which they support pattern separation and as they age, these cells may undergo a functional switch from pattern separation to acquiring an increased ability to trigger pattern completion-mediated recall.

EXPERIMENTAL PROCEDURES

All methods and statistics are described in detail in the Supplementary Material.

Generation of mice

DG-TeTX mice and their control littermates (Tg1xTg3-TeTX) were generated using a strategy similar to that previously described (Nakashiba et al., 2008) combined with the POMC-Cre transgenic line (Tg1) (McHugh et al., 2007). Mice were raised with drinking water containing 10 μg/ml Dox (Sigma) supplemented with 1% sucrose (Sigma) from the time of conception to weaning and then with food containing 10 mg Dox/kg (Bioserve) from weaning to adulthood.

Histological methods

Immunofluorescence was performed on cryosections or vibratome sections of tissue perfused with 4% paraformaldehyde following standard protocols.

In vitro slice physiology

Field excitatory postsynaptic potentials were measured in 300-μm-thick hippocampal slices with MF, PP or RC stimulation. Whole-cell patch clamp recordings were performed from young adult-born GCs in hippocampal slices of mice injected by Moloney virus.

Moloney virus generation and injection

The Moloney virus was generated in transfected 293T cells following standard protocols (Lois et al., 2002). Concentrated viral aliquots (0.9 μl, approximately 10^9 infectious units/ml) were injected into the DG at the following sites (in mm): AP=-2.06 and ML=+1.25 from bregma, DV=-1.75 from the brain surface; AP=-2.70 and ML=+2.00 from bregma, DV=-1.75 from the brain surface.

Behavioral experiments

Hippocampal-dependent behavioral tasks included contextual discrimination (McHugh et al., 2007), eight-arm radial maze (Clelland et al., 2009), pre-exposure-dependent contextual fear conditioning (Nakashiba et al., 2008) and Morris water maze (Nakazawa et al., 2002; Slutsky et al., 2010).

In vivo electrophysiology

Control (N=14) and DG-TeTX mice (N=18) were familiarized to one of the two environments for 3 days. On testing day 4, putative neurons from the CA1 and CA3 regions of the hippocampus were recorded while animals explored the familiar environment for 15 min, followed by the presentation of the contrasting novel environment for 15 min. Before and after each RUN session, mice were placed in a small “SLEEP” box separate from the recording arenas for 20 min. The presentation of arenas was randomized between animals.

Statistical analysis

All data are presented as mean ± SEM. Comparisons between two-group data were analyzed by Student's t-test. If the data did not meet the assumptions of the t-test, the data were analyzed using the non-parametric Mann-Whitney U-test. Multiple group comparisons were assessed using a two-way or repeated-measures analysis of variance (ANOVA), followed by the Bonferroni's post-hoc test when necessary. Discrimination training was analyzed for each trial block within each genotype using Scheffé's method to correct for multiple comparisons, with a protection significance level of p=0.05. The null hypothesis was rejected at the p<0.05 level.

Supplementary Material

Refer to Web version on PubMed Central for supplementary material.

Acknowledgments

We wish to thank F. Bushard, A. Ogawa, J. Derwin, C. Lovett, D. Rooney, C. Twiss, M. Pfau and M. Serock for excellent technical assistance, Tonegawa lab members including J. Biedenkapp, J. Young and G. Dragoi for comments on earlier versions of the manuscript, N. Arzoumanian for help with manuscript preparation, C. Lois for plasmids, I. Wickersham and H.S. Seung for the rabies virus, and S. Lee for help with preliminary irradiation experiments. This work was supported by the Howard Hughes Medical Institute, Otsuka Maryland Research Institute, the Picower Foundation, and NIH grants R01-MH078821 and P50-MH58880 to S.T.; NIH grant R01-MH62122 to M.S.F.; and NICHD intramural funding to C.J.M.

References

Altman J, Bayer SA. Migration and distribution of two populations of hippocampal granule cell precursors during the perinatal and postnatal periods. J Comp Neurol. 1990; 301:365–381. [PubMed: 2262596]

Altman J, Das GD. Autoradiographic and histological evidence of postnatal hippocampal neurogenesis in rats. J Comp Neurol. 1965; 124:319–335. [PubMed: 5861717]

Amaral DG, Ishizuka N, Claiborne B. Neurons, numbers and the hippocampal network. Prog Brain Res. 1990; 83:1–11. [PubMed: 2203093]

Bakker A, Kirwan CB, Miller M, Stark CEL. Pattern separation in the human hippocampal CA3 and dentate gyrus. Science. 2008; 319:1640–1642. [PubMed: 18356518]

Braz JM, Rico B, Basbaum AI. Transneuronal tracing of diverse CNS circuits by Cre-mediated induction of wheat germ agglutinin in transgenic mice. PNAS U S A. 2002; 99:15148–15153.

Burgess N, Maguire EA, O'Keefe J. The human hippocampus and spatial and episodic memory. Neuron. 2002; 35:625–641. [PubMed: 12194864]

Clelland CD, Choi M, Romberg C, Clemenson GD, Fragniere A, Tyers P, Jessberger S, Saksida LM, Barker RA, Gage FH, et al. A functional role for adult hippocampal neurogenesis in spatial pattern separation. Science. 2009; 325:210–213. [PubMed: 19590004]

Creer DJ, Romberg C, Saksida LM, Praag H van, Bussey TJ. Running enhances spatial pattern separation in mice. PNAS USA. 2010; 107:2367–2372. [PubMed: 20133882]

Eriksson PS, Perfilieva E, Björk-Eriksson T, Alborn AM, Nordborg C, Peterson DA, Gage FH. Neurogenesis in the adult human hippocampus. Nat Med. 1998; 4:1313–1317. [PubMed: 9809557]

Fanselow M. Associative vs topographical accounts of the immediate shock-freezing deficit in rats: Implications for the response selection rules governing species-specific defensive reactions. Learning and Motivation. 1986; 17:16–39.

Fanselow M. Factors governing one-trial contextual conditioning. Animal Learning & Behavior. 1990; 18:264–270.

Ge S, Yang C-H, Hsu K-S, Ming G-L, Song H. A critical period for enhanced synaptic plasticity in newly generated neurons of the adult brain. Neuron. 2007; 54:559–566. [PubMed: 17521569]

Gilbert PE, Kesner RP, Lee I. Dissociating hippocampal subregions: double dissociation between dentate gyrus and CA1. Hippocampus. 2001; 11:626–636. [PubMed: 11811656]

Gould E, Beylin A, Tanapat P, Reeves A, Shors TJ. Learning enhances adult neurogenesis in the hippocampal formation. Nat Neurosci. 1999; 2:260–265. [PubMed: 10195219]

Hasselmo ME, Schnell E, Barkai E. Dynamics of learning and recall at excitatory recurrent synapses and cholinergic modulation in rat hippocampal region CA3. J Neurosci. 1995; 15:5249–5262. [PubMed: 7623149]

Hunsaker MR, Kesner RP. Evaluating the differential roles of the dorsal dentate gyrus, dorsal CA3, and dorsal CA1 during a temporal ordering for spatial locations task. Hippocampus. 2008; 18:955–964. [PubMed: 18493930]

Imayoshi I, Sakamoto M, Ohtsuka T, Takao K, Miyakawa T, Yamaguchi M, Mori K, Ikeda T, Itohara S, Kageyama R. Roles of continuous neurogenesis in the structural and functional integrity of the adult forebrain. Nat Neurosci. 2008; 11:1153–1161. [PubMed: 18758458]

Jung MW, McNaughton BL. Spatial selectivity of unit activity in the hippocampal granular layer. Hippocampus. 1993; 3:165–182. [PubMed: 8353604]

Kee N, Teixeira CM, Wang AH, Frankland PW. Preferential incorporation of adult-generated granule cells into spatial memory networks in the dentate gyrus. Nat Neurosci. 2007; 10:355–362. [PubMed: 17277773]

Kesner RP. A behavioral analysis of dentate gyrus function. Prog Brain Res. 2007; 163:567–576. [PubMed: 17765738]

Laplagne DA, Espósito MS, Piatti VC, Morgenstern NA, Zhao C, Praag H van, Gage FH, Schinder AF. Functional convergence of neurons generated in the developing and adult hippocampus. PLoS Biol. 2006; 4:e409. [PubMed: 17121455]

Lee I, Kesner RP. Encoding versus retrieval of spatial memory: double dissociation between the dentate gyrus and the perforant path inputs into CA3 in the dorsal hippocampus. Hippocampus. 2004; 14:66–76. [PubMed: 15058484]

Leutgeb JK, Leutgeb S, Moser M-B, Moser EI. Pattern separation in the dentate gyrus and CA3 of the hippocampus. Science. 2007; 315:961–966. [PubMed: 17303747]

Lois C, Hong EJ, Pease S, Brown EJ, Baltimore D. Germline transmission and tissue-specific expression of transgenes delivered by lentiviral vectors. Science. 2002; 295:868–872. [PubMed: 11786607]

Marr D. Simple memory: a theory for archicortex. Philos Trans R Soc Lond, B, Biol Sci. 1971; 262:23–81. [PubMed: 4399412]

Matus-Amat P, Higgins EA, Barrientos RM, Rudy JW. The role of the dorsal hippocampus in the acquisition and retrieval of context memory representations. J Neurosci. 2004; 24:2431–2439. [PubMed: 15014118]

McHugh T, Jones MW, Quinn JJ, Balthasar N, Coppari R, Elmquist JK, Lowell BB, Fanselow MS, Wilson MA, Tonegawa S. Dentate gyrus NMDA receptors mediate rapid pattern separation in the hippocampal network. Science. 2007; 317:94–99. [PubMed: 17556551]

McNaughton BL, Morris RGM. Hippocampal synaptic enhancement and information storage within a distributed memory system. Trends in Neuroscience. 1987; 10:408–415.

Nacher J, Crespo C, McEwen BS. Doublecortin expression in the adult rat telencephalon. Eur J Neurosci. 2001; 14:629–644. [PubMed: 11556888]

Nakashiba T, Young JZ, Mchugh TJ, Buhl DL, Tonegawa S. Transgenic inhibition of synaptic transmission reveals role of CA3 output in hippocampal learning. Science. 2008; 319:1260–1264. [PubMed: 18218862]

Nakazawa K, Quirk MC, Chitwood RA, Watanabe M, Yeckel MF, Sun LD, Kato A, Carr CA, Johnston D, Wilson MA, et al. Requirement for hippocampal CA3 NMDA receptors in associative memory recall. Science. 2002; 297:211–218. [PubMed: 12040087]

O'Reilly RC, McClelland JL. Hippocampal conjunctive encoding, storage, and recall: avoiding a trade-off. Hippocampus. 1994; 4:661–682. [PubMed: 7704110]

Overstreet LS, Hentges ST, Bumaschny VF, Souza FSJ, de Smart JL, Santangelo AM, Low MJ, Westbrook GL, Rubinstein M. A transgenic marker for newly born granule cells in dentate gyrus. J Neurosci. 2004; 24:3251–3259. [PubMed: 15056704]

Sahay A, Scobie KN, Hill AS, O'Carroll CM, Kheirbek MA, Burghardt NS, Fenton AA, Dranovsky A, Hen R. Increasing adult hippocampal neurogenesis is sufficient to improve pattern separation. Nature. 2011; 472:466–470. [PubMed: 21460835]

Santarelli L, Saxe M, Gross C, Surget A, Battaglia F, Dulawa S, Weisstaub N, Lee J, Duman R, Arancio O, et al. Requirement of hippocampal neurogenesis for the behavioral effects of antidepressants. Science. 2003; 301:805–809. [PubMed: 12907793]

Schlessinger AR, Cowan WM, Gottlieb DI. An autoradiographic study of the time of origin and the pattern of granule cell migration in the dentate gyrus of the rat. J Comp Neurol. 1975; 159:149–175. [PubMed: 1112911]

Schmidt-Hieber C, Jonas P, Bischofberger J. Enhanced synaptic plasticity in newly generated granule cells of the adult hippocampus. Nature. 2004; 429:184–187. [PubMed: 15107864]

Scobie KN, Hall BJ, Wilke SA, Klemenhagen KC, Fujii-Kuriyama Y, Ghosh A, Hen R, Sahay A. Krüppel-like factor 9 is necessary for late-phase neuronal maturation in the developing dentate gyrus and during adult hippocampal neurogenesis. J Neurosci. 2009; 29:9875–9887. [PubMed: 19657039]

Scoville WB, Milner B. Loss of recent memory after bilateral hippocampal lesions. J Neurol Neurosurg Psychiatr. 1957; 20:11–21. [PubMed: 13406589]

Slutsky I, Abumaria N, Wu L-J, Huang C, Zhang L, Li B, Zhao X, Govindarajan A, Zhao M-G, Zhuo M, et al. Enhancement of learning and memory by elevating brain magnesium. Neuron. 2010; 65:165–177. [PubMed: 20152124]

Snyder JS, Choe JS, Clifford MA, Jeurling SI, Hurley P, Brown A, Kamhi JF, Cameron HA. Adult-born hippocampal neurons are more numerous, faster maturing, and more involved in behavior in rats than in mice. J Neurosci. 2009; 29:14484–14495. [PubMed: 19923282]

Squire LR, Stark CEL, Clark RE. The medial temporal lobe. Annu Rev Neurosci. 2004; 27:279–306. [PubMed: 15217334]

Tabuchi K, Sawamoto K, Suzuki E, Ozaki K, Sone M, Hama C, Tanifuji-Morimoto T, Yuasa Y, Yoshihara Y, Nose A, et al. GAL4/UAS-WGA system as a powerful tool for tracing Drosophila transsynaptic neural pathways. J Neurosci Res. 2000; 59:94–99. [PubMed: 10658189]

Tashiro A, Makino H, Gage FH. Experience-specific functional modification of the dentate gyrus through adult neurogenesis: a critical period during an immature stage. J Neurosci. 2007; 27:3252–3259. [PubMed: 17376985]

Toni N, Laplagne DA, Zhao C, Lombardi G, Ribak CE, Gage FH, Schinder AF. Neurons born in the adult dentate gyrus form functional synapses with target cells. Nat Neurosci. 2008; 11:901–907. [PubMed: 18622400]

Treves A, Rolls ET. Computational analysis of the role of the hippocampus in memory. Hippocampus. 1994; 4:374–391. [PubMed: 7842058]

Tronel S, Belnoue L, Grosjean N, Revest J-M, Piazza P-V, Koehl M, Abrous DN. Adult-born neurons are necessary for extended contextual discrimination. Hippocampus. 2010 Epub ahead of print.

van Praag H, Schinder AF, Christie BR, Toni N, Palmer TD, Gage FH. Functional neurogenesis in the adult hippocampus. Nature. 2002; 415:1030–1034. [PubMed: 11875571]

Weisskopf MG, Castillo PE, Zalutsky RA, Nicoll RA. Mediation of hippocampal mossy fiber long-term potentiation by cyclic AMP. Science. 1994; 265:1878–1882. [PubMed: 7916482]

Wickersham IR, Lyon DC, Barnard RJO, Mori T, Finke S, Conzelmann K-K, Young JAT, Callaway EM. Monosynaptic restriction of transsynaptic tracing from single, genetically targeted neurons. Neuron. 2007; 53:639–647. [PubMed: 17329205]

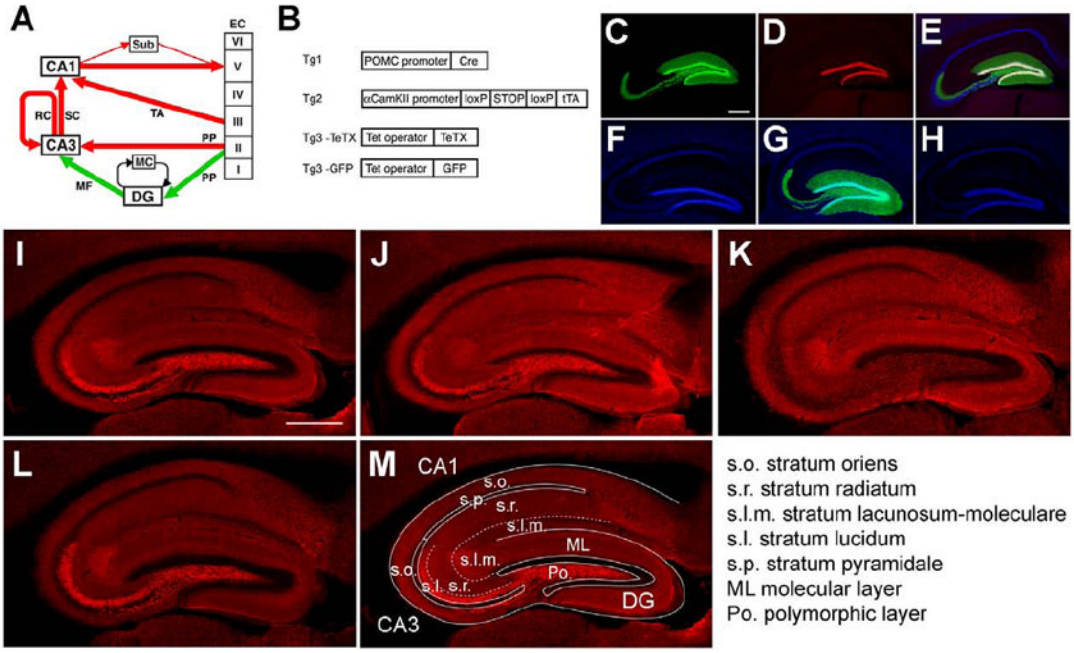

Figure 1. Application of the DICE-K method to the MF pathway

(**A**) Excitatory pathways in the hippocampus and EC. Red and green colors designate alternative pathways. (**B**) Transgenic constructs. For the production of the DG-TeTX mouse and the model mouse (DG-GFP), Tg1, Tg2 and Tg3-TeTX mice and Tg1, Tg2 and Tg3-GFP mice were crossed, respectively. (**C** to **E**) A hippocampal section from a DG-GFP mouse raised on Dox, followed by a 2-week Dox withdrawal, co-stained with anti-GFP (green), anti-Prox1 [a marker for DG GCs (red)] and anti-NeuN [a marker for neurons (blue)]. Images through a green filter (**C**), through a red filter (**D**) and through all three filters (**E**). (**F** to **H**) Hippocampal sections co-stained with anti-GFP (green) and DAPI [a marker for cell nuclei (blue)] from a chronically repressed (Dox-on) DG-GFP mouse (**F**), from a mouse after a 2-week Dox withdrawal (**G**) and from a mouse in which withdrawal was followed by a 3-week Dox readministration (**H**). (**I** to **L**) Hippocampal sections stained with anti-VAMP2 from control (**I**) and DG-TeTX mice (**J**) both raised on Dox; from a DG-TeTX mouse raised on Dox, followed by a 4-week Dox withdrawal (**K**) and further followed by a 4-week Dox readministration (**L**). (**M**) Locations of various hippocampal strata. Scale bars, 500 μm. See also Figure S1.

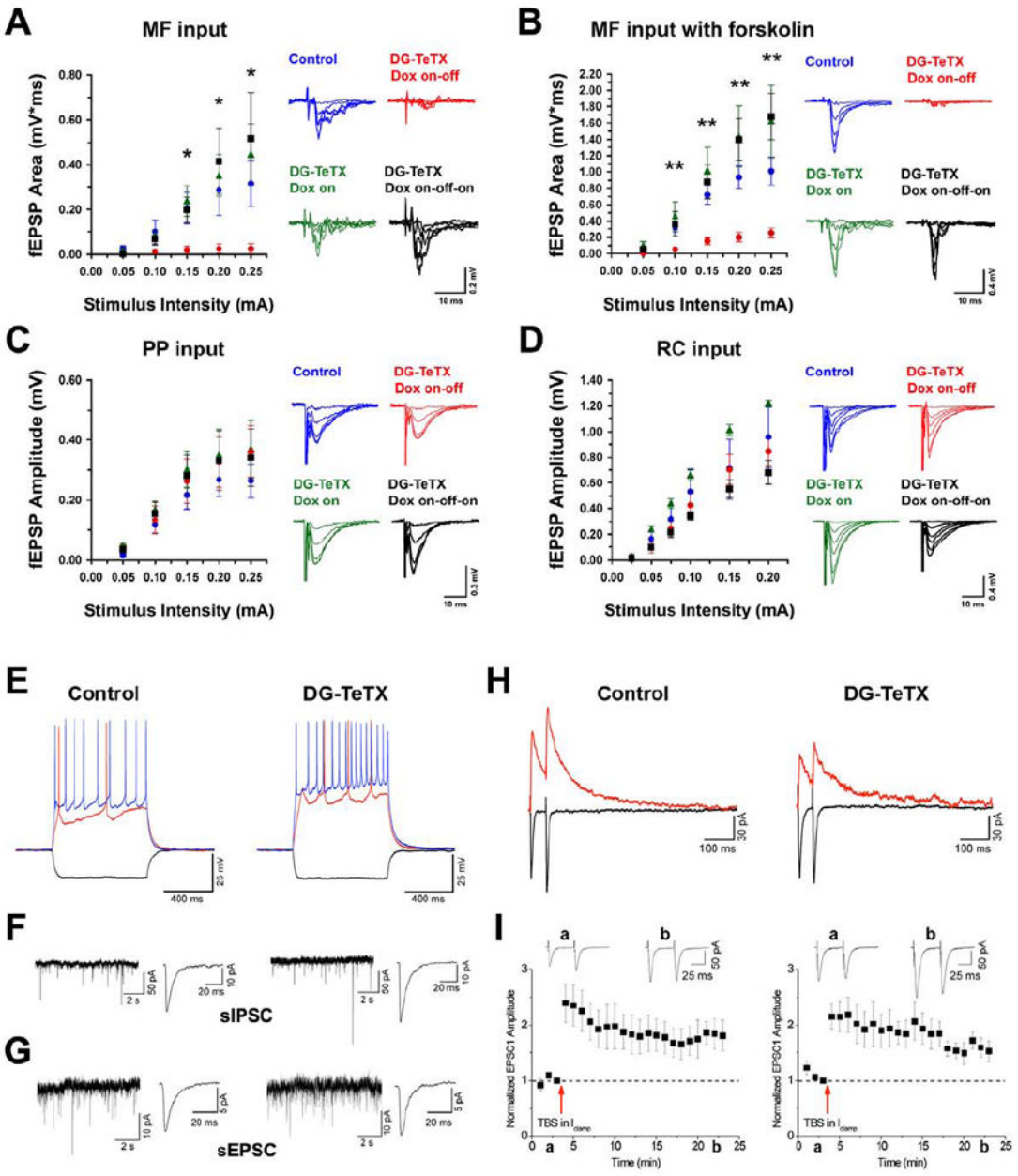

Figure 2. Blockade of MF synaptic transmission in DG-TeTX mice and comparison of firing and synaptic properties of young adult-born GCs in control and activated DG-TeTX mice

(**A** and **B**) Input-output (I-O) relationships of MF input to CA3 in control ACSF (**A**) and in the presence of forskolin (**B**). (**C**) I-O relationships of the PP input to CA3. (**D**) I-O relationships of the RC input to CA3. Blue, control littermates (Tg1xTg3-TeTX) raised under Dox-on conditions, followed by a 6-week Dox withdrawal; green, repressed DG-TeTX mice (always Dox-on); red, activated DG-TeTX mice raised under Dox-on conditions, followed by a 6-week Dox withdrawal; black, DG-TeTX mice raised under Dox-on conditions, followed by a 6-week Dox withdrawal, followed by a 4-week Dox readministration. For all I-O relations shown, n=4-7 from at least four different mice per genotype/condition. Representative traces for each condition and pathway are indicated on the right. *p<0.05, **p<0.01 between control and activated DG-TeTX mice (t-test). (**E** to **I**)

Firing and synaptic properties of young (3- to 4-week-old) adult-born GCs in control and activated DG-TeTX mice. **(E)** Representative traces showing membrane and firing properties of young GCs to hyperpolarizing (-50 pA; black traces) and depolarizing (+50 and +100 pA, red and blue traces, respectively) current injections. (**F** and **G**)Representative gap-free traces of pharmacologically isolated spontaneous $GABA_A$ and AMPA receptor-mediated IPSCs (**F**) and EPSCs (**G**) with ensemble averages (right traces) in young GCs. **(H)** Paired pulse (50 ms inter-stimulus interval) PP-evoked EPSCs at a holding potential of -70mV (black traces, AMPAR-mediated current) and at a holding potential of +40 mV (red traces, NMDAR-mediated current) in representative recordings from young GCs. (**I**) Pooled data showing long-term potentiation of PP-evoked AMPAR-mediated EPSCs in response to a theta burst induction protocol (see Experimental Procedures) in young GCs in control (n=8) and activated DG-TeTX mice (n=6). Inset traces a and b show EPSCs taken at the time indicated on the x-axes. Data represent mean ± SEM. See also Figure S2 and Table S1.

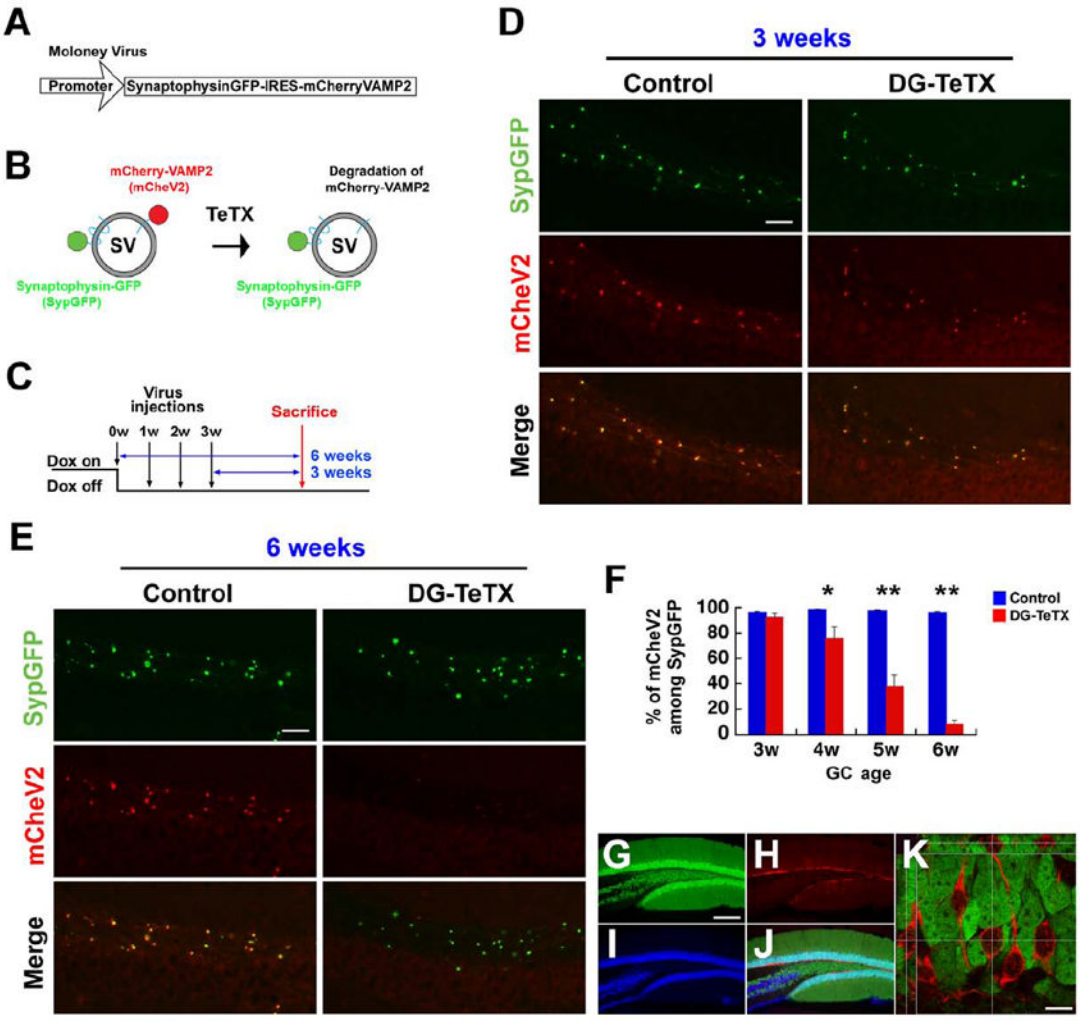

Figure 3. Integrity of MF transmission from young adult-born GCs

(**A**) A Moloney viral vector encoding bicistronic SypGFP and mCheV2. (**B**) SypGFP- and mCheV2-labeled synaptic vesicles (SV). TeTX cleaves the mCheV2, leading to the loss of mCheV2 immunoreactivity. (**C**) Dox diet, viral injection and mouse sacrifice schedules. (**D** and **E**) Presence of VAMP2 at MF boutons from 3-week-old adult-born GCs (**D**) and its absence at MF boutons from 6-week-old adult-born GCs (**E**). S. lucidum areas of hippocampal sections stained with anti-GFP (green) and anti-mCherry (red) from control and activated DG-TeTX mice. (**F**) Proportion of mCheV2-positive puncta among sypGFP-positive puncta at various GC ages. At least three different mice per genotype/condition were used. *p<0.05 for 4-week-old GCs; **p<0.01 for 5- and 6-week-old GCs (t-test). (**G** to **K**) A hippocampal section from a DG-GFP mouse co-stained with anti-GFP (green, **G**), anti-DCX (red, **H**) and anti-NeuN (blue, **I**; merge, **J**). (**K**) A confocal image at a single z-axis with green and red filters. Optical sections along the horizontal or vertical lines across multiple z-axes are shown on the top and left, respectively. Scale bar in **D** and **E**, 25 μm; **G-J**, 250 μm; **K**, 10 μm. Data represent mean ± SEM. See also Figure S3.

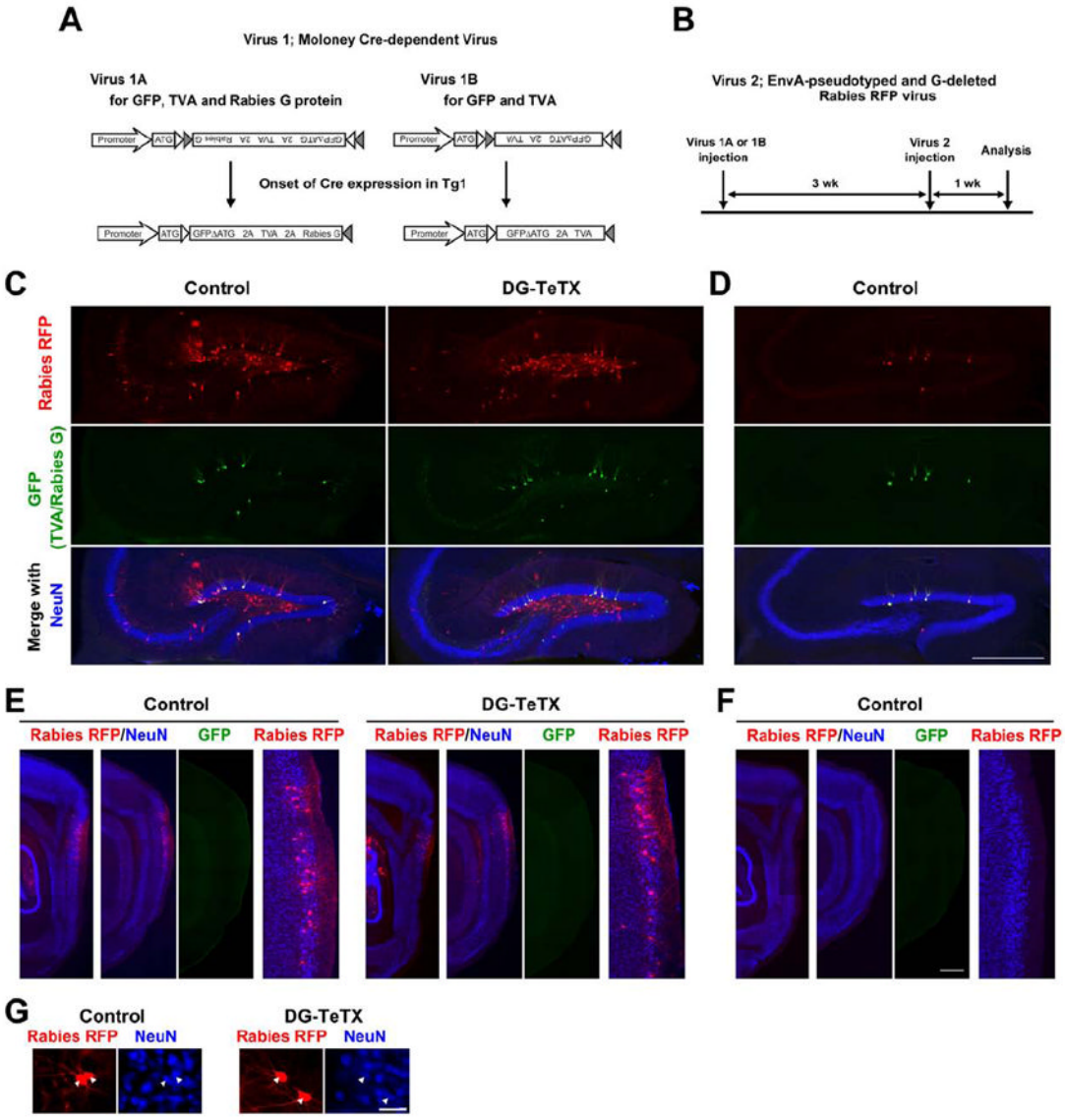

Figure 4. Young adult-born GCs receive synaptic inputs

(**A**) Two different Cre-dependent Moloney viral vectors. Virus 1A (left) expresses GFP, TVA (a receptor for EnvA) and rabies G glycoprotein, whereas Virus 1B (right) expresses GFP and TVA. Cre-loxP recombination by Tg1 occurs between 1 and 2 weeks after the Moloney virus injection (Figure S4). **(B)** Schedule of analysis relative to viral injections. (**C**) Hippocampal sections from control and activated DG-TeTX mice injected with Virus 1A and Virus 2 co-stained with anti-RFP (red), anti-GFP (green) and anti-NeuN (blue). (**D**) A hippocampal section from a control mouse injected with Virus 1B and Virus 2. (**E**) Parasagittal sections at two different medio-lateral levels covering the EC (first and second columns) from control and activated DG-TeTX mice injected with Virus 1A and Virus 2. GFP images (third column) taken from sections shown in the second column. High magnification images of the EC superficial layers (fourth column) are from images in the second column. (**F**) Parasagittal sections from a control mouse injected with Virus 1B and Virus 2. (**G**) RFP- and NeuN-positive cells (arrowheads) in the EC. Scale bars in **C-F**, 500 μm; **G**, 50 μm. See also Figure S4.

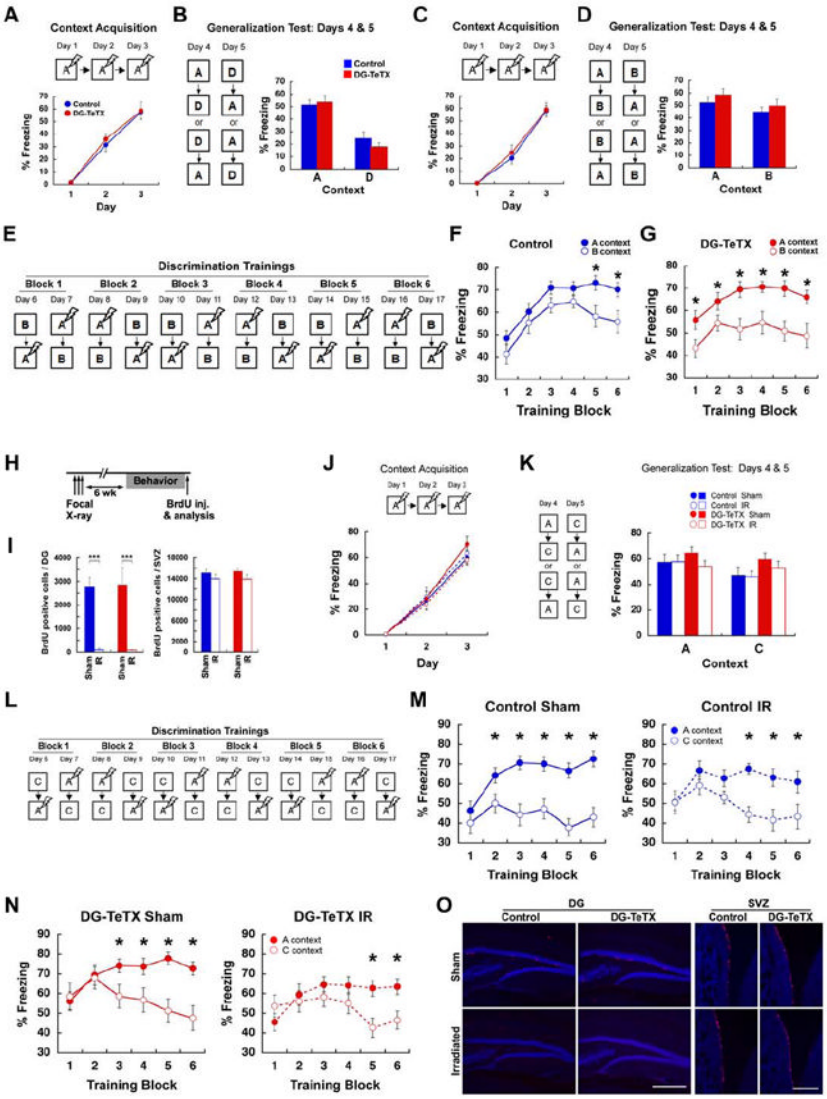

Figure 5. DG-TeTX mice show enhanced contextual discrimination in a highly similar context pair and their intact young GCs are necessary for this discrimination

(**A** and **B**) Contextual discrimination between a very distinct context pair, A and D. (**A**) Freezing levels during the acquisition (blue, control; red, DG-TeTX; *n*=12 per genotype). (**B**) Freezing levels in A and D during the generalization test. (**C** to **G**) Another set of mice (*n*=12 per genotype) were subjected to contextual discrimination between a very similar context pair, A and B. (**C**) Freezing levels during the acquisition. (**D**) Freezing levels in A and B during the generalization test. (**E**) Experimental procedure for discrimination training between A and B. (**F** and **G**) Freezing levels in A (filled circles) and B (open circles) of control (blue, **F**) and DG-TeTX mice (red, **G**). (**H** to **O**) Activated DG-TeTX and control littermates with either IR or Sham (*n*=14 per group) were subjected to contextual discrimination between a slightly distinct context pair, A and C. (**H**) Mice were focally irradiated 6 weeks prior to contextual discrimination fear conditioning. (**I**) The number of BrdU-positive cells in the DG and in the subventricular zone (SVZ; blue, control; red, DG-TeTX; ***$p<0.001$ in both genotypes, t-test). (**J**) Freezing levels during the acquisition (blue, control; red, DG-TeTX; filled circles and solid lines, Sham; open circles and broken lines, IR). (**K**) Freezing levels in A and C during the generalization test. (**L**) Experimental

procedure for discrimination trainings between A and C. (**M** and **N**) Freezing levels in A (filled circles) and C (open circles) of control (**M**) and DG-TeTX mice (**N**). (**O**) DG and SVZ area of sections stained with anti-BrdU (red) and anti-NeuN (blue). * indicates Scheffé's correction for multiple comparison, $p<0.05$. Scale bars in **O**, 500 μm. Data represent mean ± SEM. See also Figure S5.

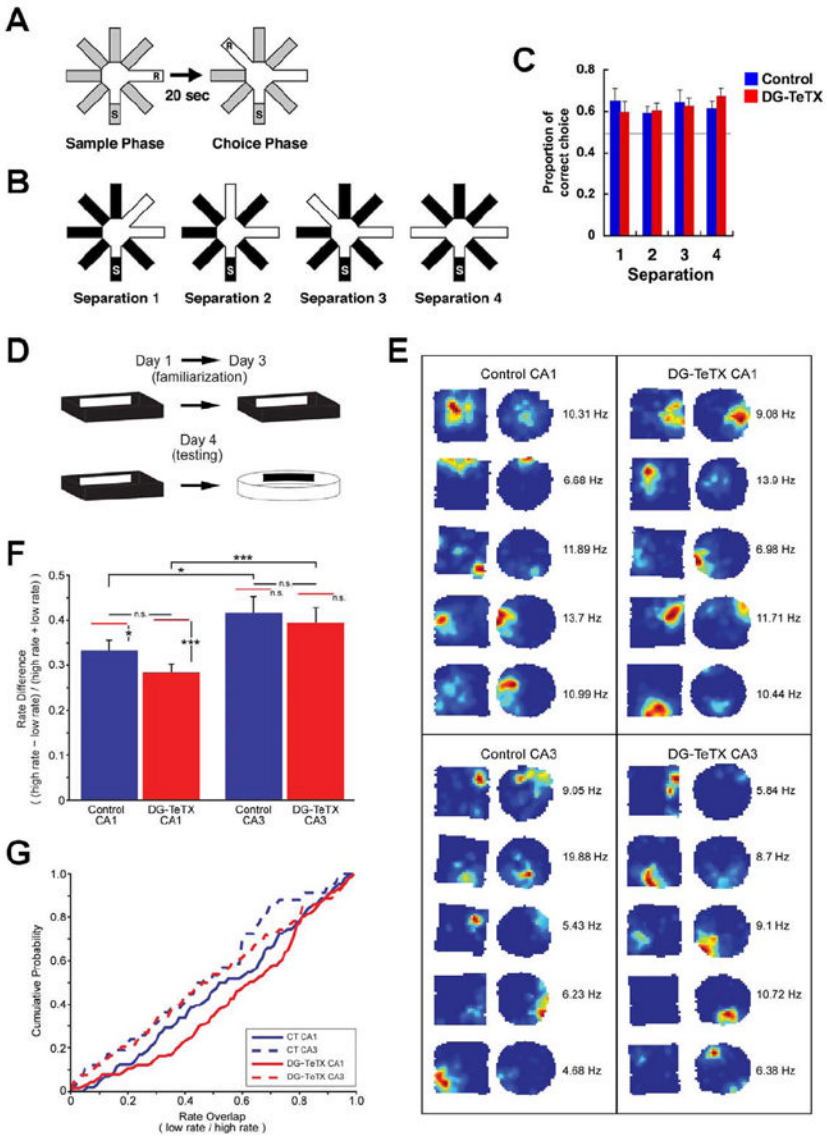

Figure 6. Normal spatial discrimination and normal rate remapping in DG-TeTX mice

(**A**) Pattern separation was tested using a DNMP protocol by varying angles between sample and reward arms (S, start arm; R, reward; see Experimental Procedures). (**B**) Two arms were separated by 45°, 90°, 135° and 180° in separation 1-4, respectively. (**C**) Proportions of correct choices as a function of arm separation angles. The horizontal gray line represents chance. *n*=12 per genotype. (**D**) Example of behavioral pattern separation paradigm. (**E**) Place field examples from control (left) and DG-TeTX mice (right) for CA1 (top) and CA3 (bottom) pyramidal cells. The two maps from each example were normalized to the maximum peak firing rate between the maps, indicated to the right of each pair. (**F**) Rate remapping index for place cells recorded from CA1 (left) and CA3 (right) regions of control (blue) and DG-TeTX mice (red). There was a similar significant difference in rate between CA1 and CA3 in control and DG-TeTX mice (**p*<0.05 and ****p*<0.001, respectively, t-test). The red bars above each column represent the estimated rate difference (ERD) expected given independent firing in the two boxes for that region/genotype. Only significant differences were observed between the actual and ERD in the CA1 regions of control and DG-TeTX mice (**p*=0.012 and ****p*<0.001, respectively, t-test). (**G**)

Cumulative probability histograms of the overlap values (low rate/high rate) for each genotype and region. Data represent mean ± SEM. See also Table S2.

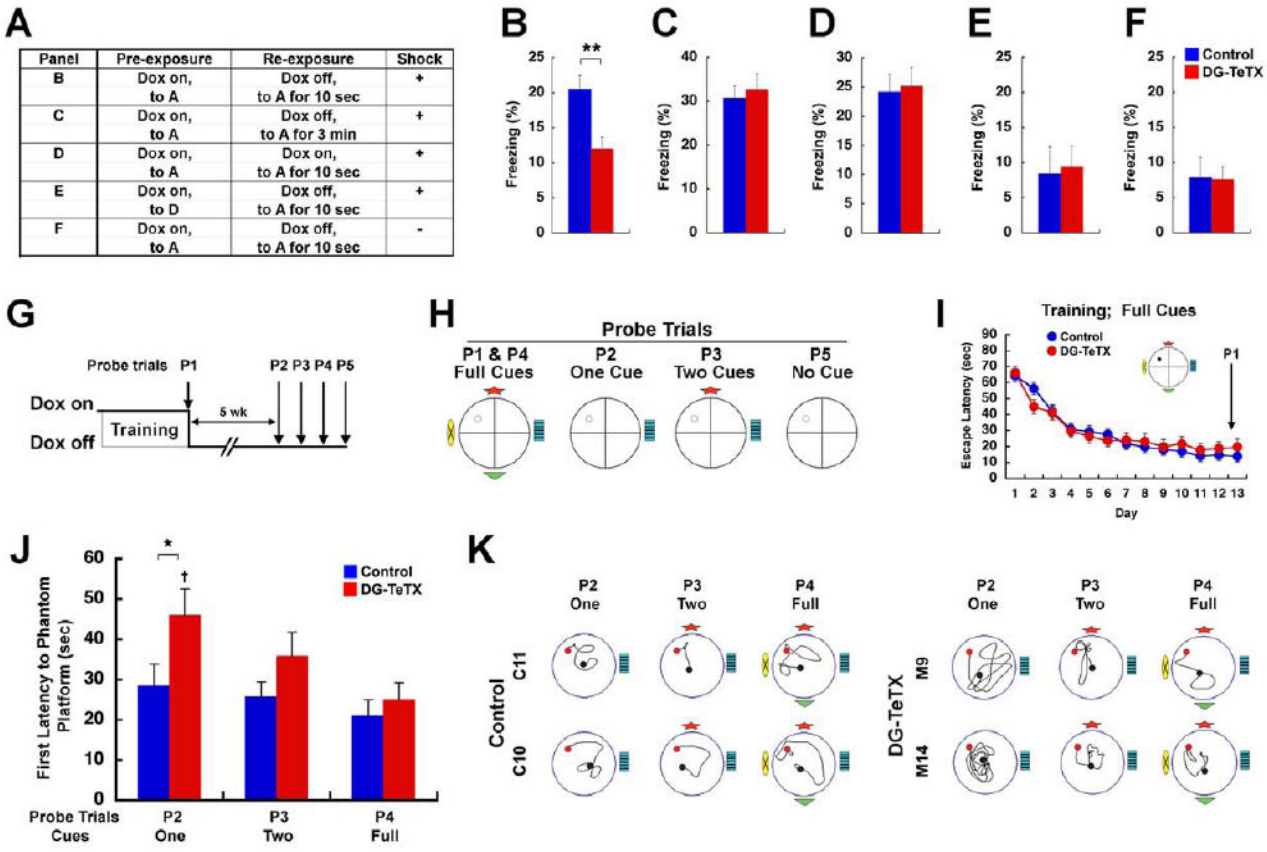

Figure 7. DG-TeTX mice exhibit deficits in pattern completion-mediated contextual and spatial recall

(**A** to **F**) Pre-exposure-dependent contextual fear conditioning. (**A**) Experimental procedure for **B** to **F**. Repressed DG-TeTX and control littermates were subjected to a pre-exposure session (for 5 consecutive days, 10 min per day) in either context A or D. The mice were then shifted to a Dox-free diet (except in **D**). Next, the mice were (re)-exposed to context A and then received a single footshock within either 10 s or 3 min. Mice in **F** did not receive a footshock. (**B** to **F**) Freezing levels in context A measured 1 day after (re)-exposure (blue, control; red, DG-TeTX). (*n*=35 and 36 in **B** for DG-TeTX mice and control mice, respectively; *n*=24, 24, 12 and 12 for both genotypes in **C, D, E** and **F**, respectively; $^{**}p<0.01$, t-test). (**G** to **K**) Spatial memory recall with various cue conditions in the standard Morris water maze task. (**G**) Experimental procedure. Repressed DG-TeTX (*n*=23) and control littermates (*n*=24) were trained to locate a hidden platform location in the full-cue condition. The mice were then switched to a Dox-free diet. The P1 probe trial was conducted under the Dox-on condition, whereas the P2-P5 probe trials were conducted under the Dox-off condition. (**H**) Probe trials with cue manipulation. (**I**) Escape latencies to the hidden platform during the training (blue, control; red, DG-TeTX). (**J**) First latencies to the phantom platform during the probe trials. (**K**) Examples of the swim path to the phantom platform (red) for the probe trials (the black circle represents the start point). $^{*}p<0.05$; $^{\dagger}p<0.01$ in DG-TeTX mice, P2 vs. P4. Data represent mean ± SEM. See also Figure S6 and S7.